Optik - International Journal for Light and Electron Optics 293 (2023) 171453

Contents lists available at ScienceDirect

Optik

journal homepage: www.elsevier.com/locate/ijleo

The performance analysis of the laser heterodyne ultra-high frequency detection based on the optical phase-locked loop

Chunhui Yan [a,b,*], Dong Yao [a,b], Lingtong Meng [a,b], Hanyu Wang [a,b], Hangang Liang [a,b], Chunming Jiang [a,b]

[a] Changchun Institute of Optics, Fine Mechanics and Physics, Chinese Academy of Science, Changchun 130033, China
[b] Key Laboratory of Airborne Optical Imaging and Measurement, Chinese Academy of Sciences, Changchun 130033, China

ARTICLE INFO

Keywords:
Laser heterodyne
Ultra-high frequency detection
Optical phase-locked loop
Residual phase variance

ABSTRACT

The performance of the laser heterodyne ultra-high frequency detection based on the optical phase-locked loop is analyzed through theoretical calculations and numerical simulations, considering the residual phase error and carrier stability. Appling the Wiener–Khinchin theorem, a general expression of the residual phase variance with essential affecting factors is derived. Furthermore, we define the error gain factor based on the ultra-high frequency carrier stability, which consists of the amplitude deviation and frequency deviation. Then the model of the demodulation output with the amplitude deviation and frequency deviation is presented. According to numerical simulation results, we acquired the variation curve of the residual phase variance with the loop bandwidth and the performance of the carrier signal stability. For the residual phase variance expression, the minimum variance corresponding to the optimal parameters can be obtained through the numerical simulation. The simulation experiment proves that the numerical results are consistent with the theoretical analysis. Our model for evaluating the influence of the carrier stability on the heterodyne ultra-high frequency detection can provide powerful support for improving the demodulation accuracy. The quantitative analysis of the paper will be available for theoretical basis and guidance for laser heterodyne detection based on optical phase-locked loops.

1. Introduction

Laser heterodyne vibration sensors for high frequencies have been investigated since years for characterizing RF-MEMS devices such as high performance filters, switches and resonators[1,2]. The sensitive and non-contact measurement of these micro vibrations in RF-MEMS devices is critical for quality control and process optimization. Ultra-high frequency(UHF) micro-nano devices based on micro/nano-electromechanical system have an important application in many fields such as life science, mobile communication, radio frequency identification, automotive electronics[3–6]. The vibration characteristics of these devices are an important indicator of product qualification rate, so the demand for UHF vibration characteristics measurement of micro-nano devices becomes more and more urgent.

Laser Doppler vibrometers (LDV) provide a sensitive and contactless measurement technique for UHF vibrations, but are limited in GHz heterodyning by the efficiency drop of acousto-optic frequency shifters. Heterodyning by frequency-offset locking of two lasers in

* Corresponding author at: Changchun Institute of Optics, Fine Mechanics and Physics, Chinese Academy of Science, Changchun 130033, China.
E-mail address: chh_yan@sina.com (C. Yan).

https://doi.org/10.1016/j.ijleo.2023.171453
Received 24 November 2022; Received in revised form 28 September 2023; Accepted 4 October 2023
Available online 6 October 2023
0030-4026/

an optical phase-locked loop (OPLL) overcomes this limitation[7,8]. Laser heterodyne techniques based on the OPLL are well applied to UHF vibration analysis of RF-MEMS in the range of MHz to GHz[9]. As an optical non-contact measurement method, the laser Doppler UHF vibration measurement technique not only has high resolution in the order of picometers, but also can realize full bandwidth real-time response of target vibration spectrum and vibration morphology, becoming a forward technique in UHF micro vibration measurement field.

The micro-vibration measurement relies on the laser-Doppler effect, which transduces the target vibration at the measurement point into a phase modulation of the echo light. The measurement beam generates Doppler phase modulations and carries the vibration information of the target. Heterodyne detection techniques realize the spectrum shift through the carrier modulation, thus isolating the target vibration signal from the low-frequency environmental interference. Relevant researchers pursue the generation of a UHF carrier signal for laser heterodyne detection system by frequency-offset locking of two semiconductor lasers in an optical phase-locked loop[10,11]. Through high-precision feedback control of electrical signals, OPLL can realize accurate regulations of UHF carrier signals and achieve a dynamic frequency difference by the phase locking between two or more independent lasers.

Required bandwidth and center frequency are often dominated by the vibration frequency rather than by the Doppler frequency when the detection target has the vibration characteristics of UHF and small amplitude[12]. For a precise reconstruction of small vibration amplitudes, the heterodyne-carrier frequency must exceed the maximum vibration frequency of the target. Further, the electronic sampling bandwidth has to be larger than twice the maximum vibration frequency of the target to ensure that the sampled signal is not distorted. The performances of the laser heterodyne UHF detection system depend on not only the laser source, surface roughness, and the matching process of the measurement beam and local oscillator beam (the reference beam) but also the rest of the system, such as the phase-locking accuracy and demodulation algorithm.

Some researchers have presented many methods for estimating the system performance of the laser heterodyne UHF detection system. Robert Kowarsch et al. discussed the collapse of the heterodyne carrier at vanishing mutual coherence due to interferometer delays and the transition to shot-noise-limited detection[7,8]. Moritz Giesen et al. considered the influence of optical crosstalk between different measuring beams in the laser Doppler 3D vibrations measuring system[13]. Li et al. explained and analyzed the nonlinear LDV distortions caused by a strong second-order ghost reflection originating from lens flares[14]. However, there is no quantitative analysis of the residual phase error and frequency stability seen in relevant papers, which are important factors in analyzing the performance of the laser heterodyne UHF vibration measurement systems. Therefore, we presented a comprehensive model for estimating the influence of the UHF carrier instability on the laser heterodyne detection.

In this paper, we firstly introduced the laser Doppler technique and the basic structure of OPLL. The combination of two techniques can provide a dynamic carrier signal for the UHF micro vibration detection. Then we discuss the variance of the residual phase error between the phase-locked output light and the master laser, which is the principal parameter that indicates the phase-locking accuracy. Besides, we define an error gain factor consisting of the amplitude deviation and frequency deviations, which characterizes the calculated phase with the deviation. Based on the factor, we established the model of the demodulation output and investigate the influence of the carrier stability on the reconstruction of target vibration characteristics through the theoretical derivation. The numerical results and calculation conclusion have the potential application for the device parameter selection of the laser heterodyne UHF detection system based on the OPLL.

2. Laser heterodyne UHF detection

2.1. Laser Doppler technique

The laser Doppler technique is the basis of laser heterodyne UHF vibration measurement. A LDV system relies on the deterministic phase modulation caused by the temporal modulation of the optical path difference due to the laser-Doppler effect. The backscattered light of a moving target in the laser heterodyne detection system contains the information of its velocity and displacement. The instantaneous velocity of the moving target determines the Doppler frequency shift, and the modulation phase of the measurement beam depends on its displacement. The Doppler shift is generated through a variation of optical path differences. Therefore, the accurate extraction of Doppler shift is directly related to the accurate reconstruction of target vibration characteristics.

Usually, the reference beam is obtained with a beam splitter from the same laser as the measurement beam. The electrical field of the measurement beam is phase-modulated through the motion of the target. Obviously, the signal intensity on the surface of the photodetector is determined by relative phase of the heterodyning light waves. The differential phase of the photocurrent signal contains three parts: carrier phase, modulation phase caused by the target vibration and stochastic phase generated during the laser transmission. At the photodetector, the photocurrent generated by the beat signal of the measurement beam (power P_m and mean frequency f_m) and the reference beam (power P_r and frequency f_r) is written as[15,16].

$$\Delta i(t) = 2K\sqrt{P_m P_r}\cos[2\pi(f_m - f_r)t + \Delta\varphi_D(t) + \varphi_d(t)], \tag{1}$$

where $K = \eta q/h\upsilon$ is the photoelectric conversion parameter of the detector in terms of quantum efficiency η, the electron charge q, Planck's constant h, mean frequency of laser υ, the Doppler modulated phase $\Delta\varphi_D(t)$, and the phase difference between the measurement beam and the reference beam $\varphi_d(t)$. This intermediate frequency (IF) is denominated as the heterodyne carrier frequency $f_c = |f_m - f_r|$. This frequency shift is conventionally introduced by an OPLL in the laser heterodyne UHF detection system.

For a displacement $s(t)$ of the moving target (parallel to the incident measurement beam) relative to the LDV (containing sender and receiver), this modulation phase can be written as[12,17].

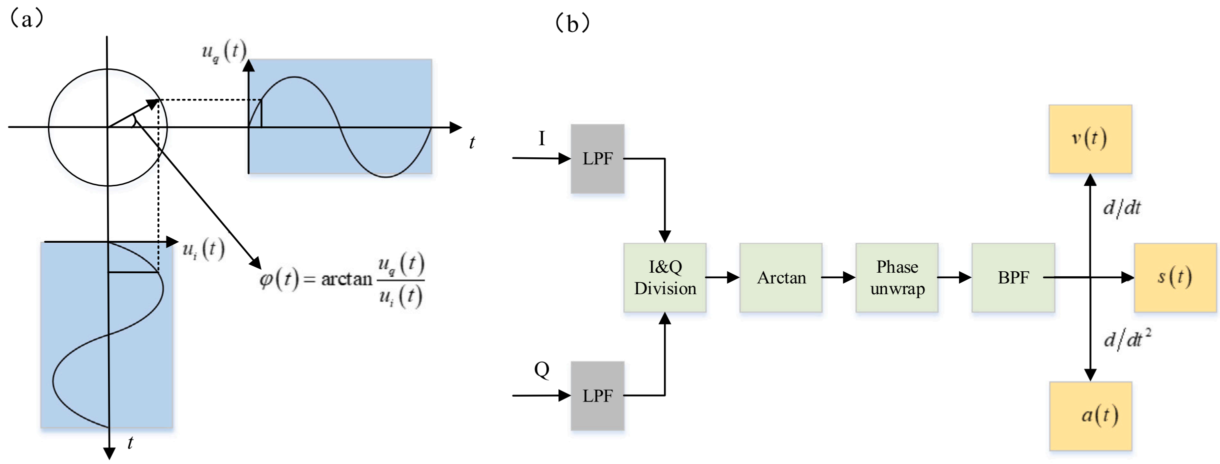

Fig. 1. The representation of the I&Q signal in a vector diagram (a) and arctangent demodulation process (b). LPF: Low-pass Filter. BPF: Band-pass Filter.

$$\Delta\varphi_D(t) = \frac{4\pi s(t)}{\lambda} \tag{2}$$

with the laser wavelength λ. This equation is also suitable for estimating the laser-Doppler effect even at ultra-high modulation frequencies. A phase modulation generates a frequency modulation at the same time. According to the fundamental relationships $d\varphi(t)/dt = 2\pi f$ and $ds(t)/dt = v(t)$, we can get the corresponding frequency shift with respect to the central frequency[12].

$$\Delta f_D = \frac{2v(t)}{\lambda}, \tag{3}$$

which is commonly referred to as the Doppler frequency shift. The velocity parameter $v(t)$ should be the radial velocity of the target parallel to the laser direction. The instantaneous frequency of the heterodyne signal correctly preserves the directional information (positive and negative signs) of the velocity vector. Therefore, we can estimate the vibration direction according to the positive or negative value of the Doppler frequency shift.

Eqs. (2) and (3) demonstrate that the vibration displacement $s(t)$ and velocity $v(t)$ of the target are encoded in the phase and frequency modulation of the detector output signal, directly related to the laser wavelength λ. In order to recover and reconstruct the vibration characteristics of the target, the phase generated carrier (PGC) technique is utilized to demodulate the photocurrent signal [18–20]. A proven standard signal decoding method for the laser heterodyne detection system relies on calculation of the phase angle by the arctangent method. The arctangent algorithm extracts the modulation phase angle through a signal pair containing in-phase (I signal, amplitude U_i) and quadrature (Q signal, amplitude U_q) components, whose voltage amplitudes depend on the interferometric phase angle $\varphi(t)$[12]:

$$\begin{cases} u_i(t) = U_i \cos\varphi(t) \\ u_q(t) = U_q \sin\varphi(t) \end{cases}. \tag{4}$$

Such a signal combination is called an I&Q baseband signal due to no frequency offset. In the baseband, the signal pair carrying the complete Doppler information is essential. Although the absolute value of displacement $s(t)$ is represented by each component, its sign can only be recovered from both signals in combination. In Fig. 1, we show the representation of the I&Q signal in a vector diagram and arctangent demodulation process. It can be inferred that the displacement $s(t)$ of the target vibration can be directly obtained by the arctangent approach. The velocity and acceleration information of the target can be recovered by first order differential and second order differential processing of the phase.

In the case of an ideal heterodyne detection, both baseband signal amplitudes are equal, i.e., $U_i = U_q$, and the relative phase shift is exactly 90°. And the I&Q format is an ideal starting for the Doppler signal decoding. Recovering the target displacement $s(t)$ simply requires the calculation of the phase angle $\varphi(t)$ from the sampled instantaneous voltage values of the I&Q signals based on the trigonometric relationship $\tan\alpha = \sin\alpha/\cos\alpha$. But in the actual situation, there is always a slight deviation because of the chip precision, the laser and optical phase-locking accuracies or the background noise. In Section 3, we will analyze the influence of this deviation on the demodulation accuracy.

2.2. The structure of optical phase-locked loop and phase-locking accuracy

The technique of heterodyning by frequency-offset locking between two or more laser sources with an OPLL has established itself in many fields of application, such as coherent optical telecommunication, coherent combining, terahertz photonics, gravitational wave

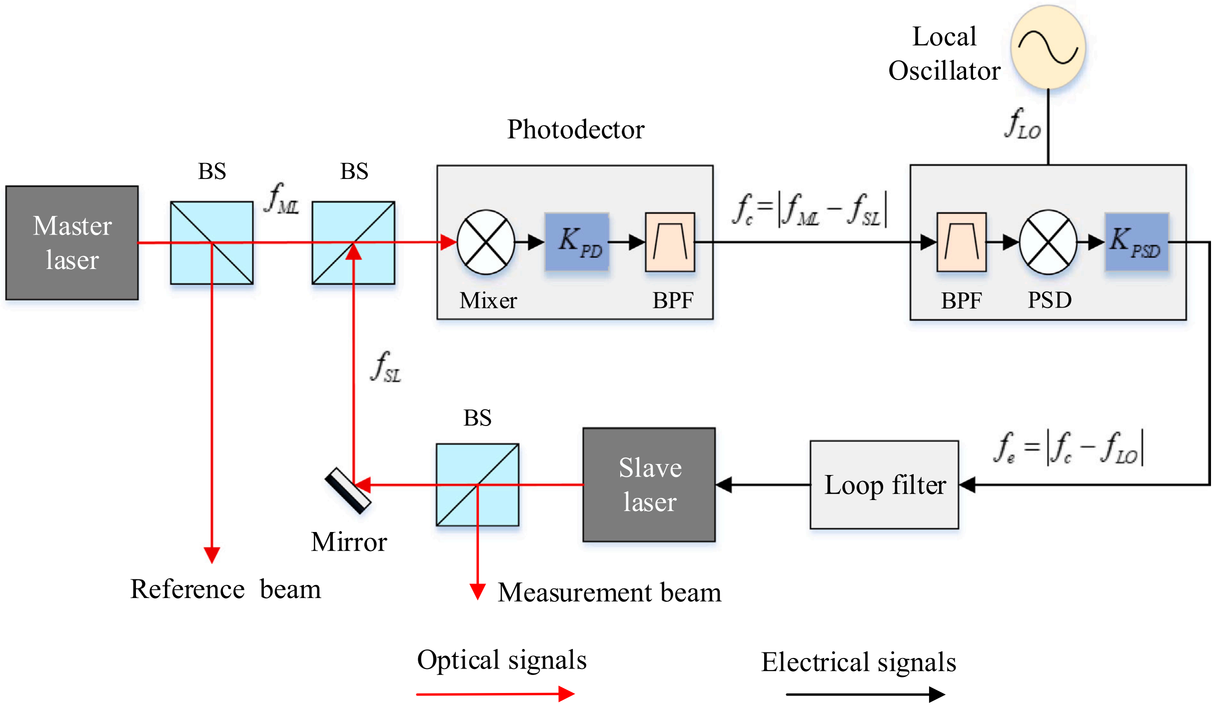

Fig. 2. The basic structure of an optical phase-locked loop in the heterodyne detection system.

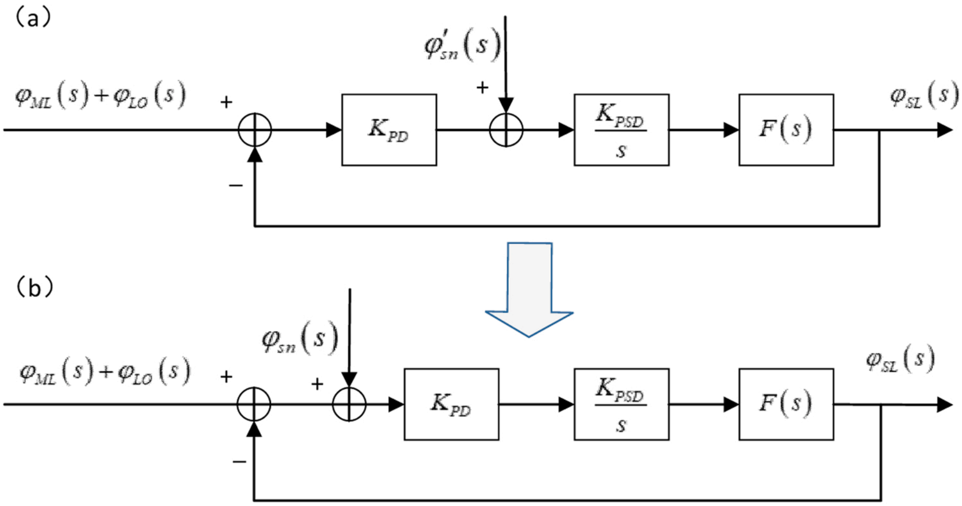

Fig. 3. The phase propagation model of the linearized OPLL. The phase of the local oscillator $\varphi_{LO}(s)$ in (a) is equivalent to the $\varphi_{sn}(s) = \varphi'_{sn}(s)/K_{PD}$ in (b).

detection and interferometry[21–24]. Heterodyning by offset-locking in an OPLL was shown in the 1960s for remote sensing and communication[25]. This optical device by frequency-offset locking can provide the ultra-high frequency carrier signal for the laser Doppler UHF detection system. The basic structure of the OPLL for the heterodyning detection is shown in Fig. 2. The optical phase-locked device mainly consists of the master laser (the reference laser), the slave laser (the measurement laser), the photodetector, the phase sensitive detector (PSD), the local oscillator and the loop filter.

BS is non-polarizing beam splitter. f_{ML} and f_{SL} are the mean frequencies of the master and slave lasers respectively. K_{PD} and K_{PSD} are the DC gain of photodetector and phase sensitive detector respectively. The photodetector detects the mixing signal between the master laser and slave laser. The phase sensitive detector compares this frequency difference to the frequency f_{LO} of the local oscillator. The frequency error f_e is fed back to the tunable slave laser by the loop filter. In lock, the frequency difference of the slave laser in respect to the master laser is locked to the frequency of the local oscillator. Thus, the local oscillator determines this frequency difference and the heterodyne carrier frequency generated by an OPLL is[7,8].

$$f_c = |f_{ML} - f_{SL}| = f_{LO}. \tag{5}$$

When the phase-locked loop works stably, the frequency of the slave laser matches the frequency of the master laser shifted by the frequency of the local oscillator. Hence, the mixing signal between the master laser and slave laser always tracks the frequency of the local oscillator. Theoretically, the frequency difference between the mixing signal and the local oscillator signal maintains dynamic stability. If the frequency of the local oscillator signal changes, the mixing signal will automatically track it within a certain frequency range under the control of the phase-locked loop and thus to achieve dynamic synchronization between the slave laser and the master laser.

The phase propagation model of the linearized OPLL is shown as Fig. 3. φ_{ML} and φ_{SL} are the phase of the master and slave lasers respectively. φ_{sn} is the phase error caused by the shot noise of photodetector. The transfer function of the filter is denoted by $F(s)$. The OPLL system can be represented by a linear system and the input signal of the linear system is the differential phase between the master laser and the slave laser. The open-loop transfer function of an OPLL in Laplace domain is[26].

$$\left.\begin{cases} G(s) = \dfrac{K_{PD}K_{PSD}F(s)}{s} \\ F(s) = K_1 + \dfrac{K_2}{s} \end{cases}\right\rangle G(s) = \frac{K_{PD}K_{PSD}(K_1 s + K_2)}{s^2}, \tag{6}$$

where K_1 is the gain coefficient of the proportional path through the filter and K_2 is the coefficient of the integral path through the filter. In order to deeply analyze the performance of phase-locked loop, we need to give the closed-loop transfer function and error transfer function[26]:

$$\begin{cases} H(s) = \dfrac{G(s)}{1+G(s)} = \dfrac{K_{PD}K_{PSD}F(s)}{s + K_{PD}K_{PSD}F(s)} \\ E(s) = 1 - H(s) = \dfrac{1}{1+G(s)} = \dfrac{s}{s + K_{PD}K_{PSD}F(s)} \end{cases}. \tag{7}$$

We quantify the performance of the OPLL in the heterodyne detection system by the variance of the residual phase error between the phase-locked optical output and the master laser. When an OPLL is in lock, the phase of the slave laser is related to the phases of the master laser and the local oscillator. In Laplace domain, the phase of the locked slave laser is given by[7].

$$\varphi_{SL}^{lock}(s) = H(s)\varphi_{ML}(s) + E(s)\varphi_{SL}(s). \tag{8}$$

In lock, the variance can be expressed in the frequency domain by the Wiener–Khinchin theorem

$$\sigma_e^2 = \int_0^{+\infty} S_\varphi^e(f)df \tag{9}$$

where $S_\varphi^e(f)$ is the power spectral density function of the variance, including three parts: the phase noise introduced by the laser, the shot noise introduced by the photodetector and the crosstalk between the data-detection- branches and phase-lock-branches of the receiver. The phase noise, the shot noise and the crosstalk processes are independent from each other. Here, the power spectral density function in the whole OPLL is given by[8,27].

$$S_\varphi^e(f) = \left|\frac{1}{1+G(s)}\right|^2 \left[S_\varphi^{ML}(f) + S_\varphi^{SL}(f)\right] + \left|\frac{G(s)}{1+G(s)}\right|^2 \left[S_\varphi^{sn}(f) + S_\varphi^{ct}(f)\right] \tag{10}$$

where $s = j2\pi f$ in steady-state, $S_\varphi^{ML}(f)$ and $S_\varphi^{SL}(f)$ are the power spectral density functions of the phase φ_{ML} and φ_{SL} respectively, $S_\varphi^{sn}(f)$ and $S_\varphi^{ct}(f)$ are the power spectral density functions of the shot noise and the crosstalk. In general, whether $S_\varphi^{ML}(f)$ or $S_\varphi^{SL}(f)$ consists of two components: white noise $S_{WN}(f)$ and flicker noise $S_{FN}(f)$. Assume that the linewidth of the master and slave lasers is $\Delta\omega$, then $S_{WN}(f)$ can be written as[28].

$$S_{WN}(f) = \frac{2\Delta\omega}{\pi f^2} \tag{11}$$

where '2' represents the sum of two laser linewidths. $S_{FN}(f)$ can be written as[28].

$$S_{FN}(f) = \frac{K_a}{f^3}. \tag{12}$$

K_a is a constant used to characterize the magnitude of the flicker noise. The power spectral density function of the shot noise in Eq. (10) is expressed as[28].

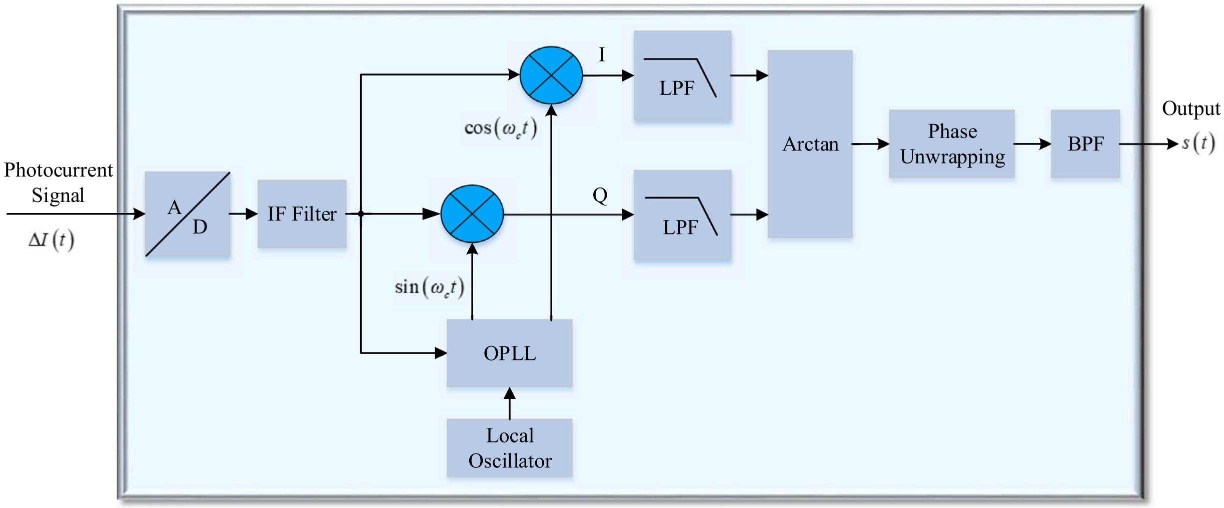

Fig. 4. The demodulation process of the IF carrier signal. A/D: Analog-to-Digital conversion.

$$S_\varphi^{sn}(f) = \frac{q}{2RP_m} \tag{13}$$

where q is the charge of an electron, R is the photodetector responsivity and P_m is the optical power of the measurement beam. And the power spectral density function of the crosstalk is given by[28].

$$S_\varphi^{ct}(f) = 2T\tan^2\varphi_{pm}\left(\frac{\sin \pi fT}{\pi fT}\right)^2 \tag{14}$$

where T is the bit duration and φ_{pm} is the phase deviation created by the phase modulator. According to the above derivation, the variance of the residual phase error can be expressed as

$$\sigma_e^2 = \int_0^{+\infty}\left[\left|\frac{1}{1+G(j2\pi f)}\right|^2\left(\frac{2\Delta\omega}{\pi f^2}+\frac{K_a}{f^3}\right)+\left|\frac{G(j2\pi f)}{1+G(j2\pi f)}\right|^2\left[\frac{q}{2RP_m}+2T\tan^2\varphi_{pm}\left(\frac{\sin \pi fT}{\pi fT}\right)^2\right]\right]df. \tag{15}$$

The OPLL noise bandwidth B_n is defined by[29,30].

$$B_n = \int_0^{+\infty}|H(j2\pi f)|^2 df = \int_0^{+\infty}\left|\frac{G(j2\pi f)}{1+G(j2\pi f)}\right|^2 df. \tag{16}$$

In general, there is a following approximate expression for a common second-order OPLL[28].

$$\sigma_e^2 \approx \frac{2.36\Delta\omega}{B_n}+\frac{8.71K_a}{B_n^2}+\frac{qB_n}{2RP_m}+\frac{2B_n\tan^2\varphi_{pm}}{R_b}. \tag{17}$$

R_b (bit/s) is the system bit rate. According to the above relationship, this proves that the variance of the residual phase error is mainly affected by four factors: the laser linewidth $\Delta\omega$, the noise bandwidth B_n, the optical power of the measurement beam P_m and the phase deviation φ_{pm} created by the phase modulator. Note that there is an optimal value B_n to minimize the variance of the residual phase error for given values of $\Delta\omega$, K_a, P_m, R_b and φ_{pm}.

The loop bandwidth defined previously is limited due to the phase-detector nonlinearity, the local oscillator fluctuations, the loop noise, etc. The input phase modulation within the loop bandwidth is tracked by the phase loop with small error. But the input phase modulation without the loop bandwidth fails to track phase modulation with almost 100% error. For the special case of the OPLL control system, the phase loop is out of lock due to excessive oscillator fluctuations or loop noise. At modulation frequencies near the loop bandwidth, error amplification occurs which impairs the stability of the OPLL.

2.3. The stability of the UHF carrier signal

The phase difference between the master laser and slave laser is compared by a mixer to the desired heterodyne carrier signal generated by the local oscillator. Obviously, the local oscillator affects the stability of the whole phase loop including the frequency stability and the amplitude stability. The frequency of the UHF carrier signal will vary with the local oscillator fluctuations. In Fig. 4, we show the demodulation process of the phase modulated signal caused by the target vibration in the laser heterodyne UHF detection system based on the OPLL. The frequency deviation of the local oscillator is transmitted in the phase of the carrier signal through the phase-locked loop system.

The frequency error $f_e = |f_c - f_{LO}|$ mentioned in Section 2.2 refers to the deviation between the frequency of the carrier signal generated by the OPLL and the designed value of the carrier frequency controlled by the local oscillator. Assume that the frequency deviation caused by local oscillator fluctuations of baseband signals I&Q is f_{ei} and f_{eq} respectively, the amplitude deviation between two baseband signals is ΔU[17].

$$\begin{cases} u_i(t) = U\cos[2\pi(f_c + f_{ei})t] \\ u_q(t) = (U + \Delta U)\sin\left[2\pi\left(f_c + f_{eq}\right)t\right] \end{cases} \tag{18}$$

where U is the amplitude of the baseband signal theoretically. From the demodulation process of the carrier signal, it can be seen that the photocurrent signal $\Delta i(t)$ is mixed by sinusoidal and cosine carrier signals respectively. Then we can use a low-pass filter to remove high-frequency components and retain low-frequency components. Two baseband signals can be expressed as

$$\begin{cases} I(t) = |[\Delta i(t) \times u_i(t)] * h_{LPF}| = K\sqrt{P_m P_r}\cdot U\cos[\Delta\varphi(t) - 2\pi f_{ei}t] \\ Q(t) = \left|\left[\Delta i(t) \times u_q(t)\right] * h_{LPF}\right| = K\sqrt{P_m P_r}\cdot (U + \Delta U)\sin\left[\Delta\varphi(t) - 2\pi f_{eq}t\right] \end{cases} \tag{19}$$

where $\Delta\varphi(t) = \frac{4\pi s(t)}{\lambda} + \varphi_d(t)$. When measuring ultra-high frequency vibrations on MEMS, the approximate formula in the reference[17] will no longer be applicable. Through the arctangent demodulation algorithm, we can get

$$\tan\Delta\varphi_{cal}(t) = \frac{Q(t)}{I(t)} = \frac{U + \Delta U}{U} \times \frac{\cos\left[\Delta\varphi(t) - 2\pi f_{eq}t\right]}{\cos[\Delta\varphi(t) - 2\pi f_{ei}t]} \times \tan\left[\Delta\varphi(t) - 2\pi f_{eq}t\right] \tag{20}$$

where $\Delta\varphi_{cal}(t)$ is the calculated value with the phase deviation. Now we define the error gain factor in the heterodyne UHF detection system based on the OPLL as

$$\delta = \frac{U + \Delta U}{U} \times \frac{\cos\left[\Delta\varphi(t) - 2\pi f_{eq}t\right]}{\cos[\Delta\varphi(t) - 2\pi f_{ei}t]} - 1. \tag{21}$$

And then the phase error due to the carrier instability can be written as

$$\begin{cases} \Delta\varphi_e = \Delta\varphi_{cal} - \Delta\varphi = -2\pi f_{eq}t + f(\delta) \\ f(\delta) = \arctan\left[\dfrac{\delta\tan\left(\Delta\varphi - 2\pi f_{eq}t\right)}{1 + (1 + \delta)\tan^2\left(\Delta\varphi - 2\pi f_{eq}t\right)}\right] \end{cases}. \tag{22}$$

First of all, we have to make it clear that the amplitude deviation ΔU is small relative to the whole amplitude of the baseband signal. The frequency deviation caused by the local oscillator fluctuation of baseband signal I&Q is approximately equal. In other words, the error gain factor δ is an infinitesimal quantity. We can expand $f(\delta)$ function by Taylor series at $\delta = 0$ to obtain

$$f(\delta) = f(0) + f'(0)\delta + \frac{1}{2}f''(0)\delta^2 + \frac{1}{6}f'''(0)\delta^3 + o\left(\delta^3\right) \tag{23}$$

where $o(\delta^3)$ represents the high-order infinitesimal of the error gain factor δ. Then we can get

$$\begin{cases} \Delta\varphi_{cal} = \Delta\varphi' + \frac{1}{2}\sin(2\Delta\varphi')\delta + \left[-\frac{1}{4}\sin(2\Delta\varphi') + \frac{1}{8}\sin(4\Delta\varphi')\right]\delta^2 + \\ \qquad \left[\frac{3}{12}\sin(2\Delta\varphi') - \frac{3}{12}\sin(4\Delta\varphi') + \frac{3}{24}\sin(6\Delta\varphi')\right]\delta^3 + o\left(\delta^3\right) \\ \Delta\varphi' = \Delta\varphi - 2\pi f_{eq}t \end{cases}. \tag{24}$$

From the theoretical derivation of the modulation phase, there are higher harmonic components associated with the error gain factor δ in the calculated value $\Delta\varphi_{cal}(t)$. Because of the frequency stability and the amplitude stability, the modulation phase is not accurate. The arctangent is an important demodulation method in the phase generated carrier technology. We can obtain the displacement $s(t)$ of the target by the arctangent demodulation algorithm. The local oscillator in the OPLL is an important source of the phase error. Therefore, we should suppress oscillator fluctuations to the greatest extent possible. Our model considers the carrier instability caused by the local oscillator, but there are other factors that make the demodulation accuracy worse, such as the laser intensity noise, the loop noise of the OPLL, laser linewidth and so on. This is also the work we need to further improve.

3. Numerical results

3.1. The variance of the residual phase error

The phase noise creates a residual phase error between the phase-locked optical received signal and the reference signal emitted by the master laser. The OPLL performance in the laser heterodyne UHF detection may be characterized by the variance of the residual

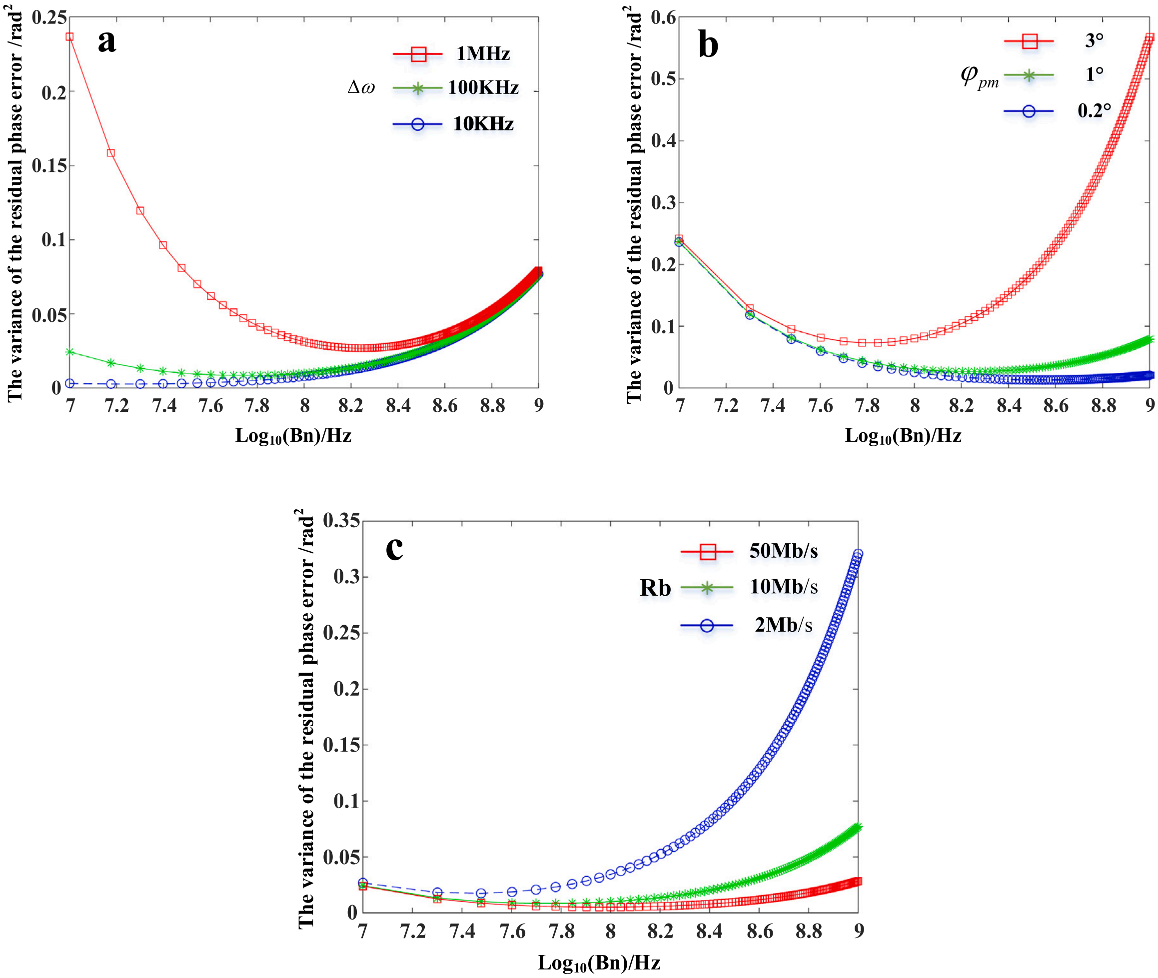

Fig. 5. The relationship between the variance of the residual phase error σ_e^2 of the optical phase-locked loop and the loop bandwidth B_n for several values of different parameters.

Table 1
The theoretical values given by the expression (17).

Parameter	Values						
$\Delta\omega$/Hz	10 K	100 K	1 M	1 M	1 M	100 K	100 K
K_a/Hz^2	5×10^8						
R/ A/W	0.5						
P_m/dBm	-50						
R_b/bit/s	10 M	10 M	10 M	10 M	10 M	2 M	50 M
φ_{pm}/°	1	1	1	0.2	3	1	1
$\sigma_{e\ \min}^2$/rad^2	2.73×10^{-3}	8.52×10^{-3}	0.027	0.0132	0.0733	0.0175	5.16×10^{-3}
$B_{n\ \min}$/Hz	1.995×10^7	5.5×10^7	1.74×10^8	3.6×10^8	6.0×10^7	2.99×10^7	8.99×10^7

phase error defined as the Eq. (9), which is related to the OPLL transfer function. With the assistance of theoretical analysis, it is known that the approximate expression of the variance of the residual phase error can be simulated by numerical results. In Fig. 5, the relationship between the variance of the residual phase error σ_e^2 of the optical phase-locked loop and the loop bandwidth B_n for several values of different parameters is shown.

According to the numerical simulation results, the variance of the residual phase error σ_e^2 increases gradually by increasing the laser linewidth $\Delta\omega$ and the phase deviation φ_{pm} created by the phase modulator. However, the variance of the residual phase error σ_e^2 decreases as the system bit rate R_b increases. For determining the parameter value of $\Delta\omega$, K_a, P_m, R_b and φ_{pm}, there is a minimum variance of the residual phase error. In this case, there is an optimal value for the loop bandwidth B_n. Table 1 lists the major design parameters given by expression (17). And we obtain the optimal values of the variance of the residual phase error σ_e^2 and the loop

Table 2
The parameters for the numerical simulations.

Parameter	Values	Unit
Photocurrent $\Delta i(t)$	1	mA
System sampling rate F_s	1000 M	Hz
Sampling time length	1×10^{-4}	s
Frequency of the Carrier Signal f_c	100 M	Hz
Frequency of the Target Vibration f_{vib}	20 M	Hz
Amplitude of the Target Vibration $\hat{v}$	1	nm
Laser Wavelength λ	1550	nm

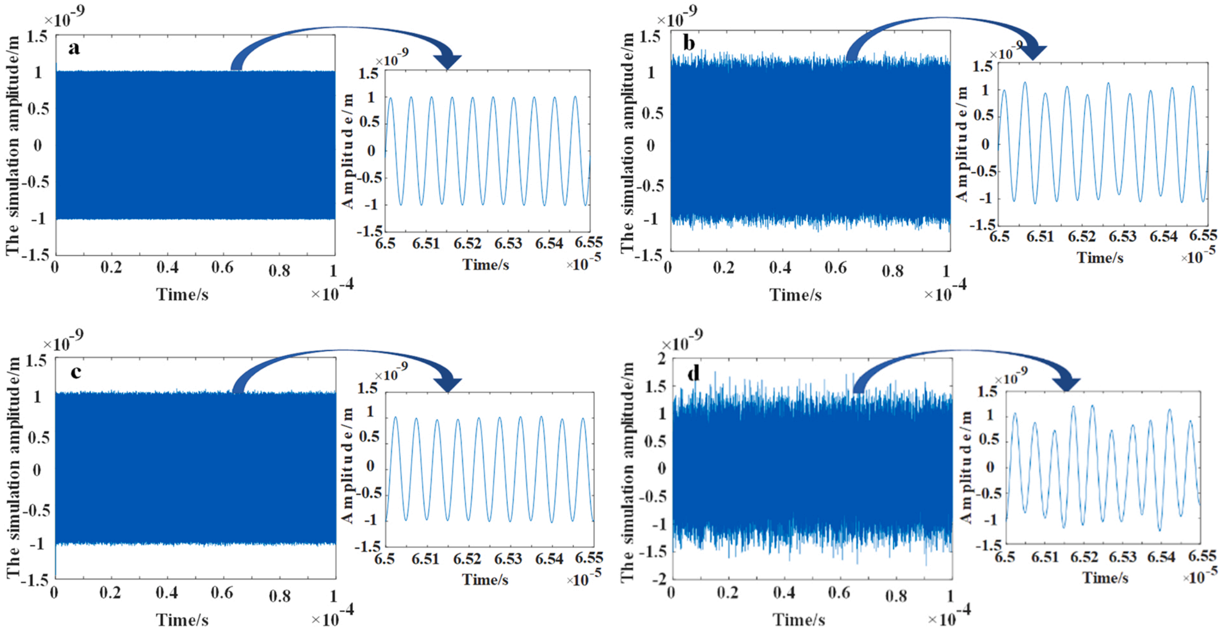

Fig. 6. The time variation curve of the demodulated output signal $s(t)$ with the different random distribution function of the amplitude deviation. (a): Random uniform distribution, $\Delta U/U = 1 \times 10^{-3}$; (b): Random uniform distribution, $\Delta U/U = 1 \times 10^{-2}$; (c): Standard normal distribution, $\Delta U/U = 1 \times 10^{-3}$; (d): Standard normal distribution, $\Delta U/U = 1 \times 10^{-2}$.

bandwidth B_n.

BER (bit error rate) is an indicator to measure the accuracy of the data transmission within a specified time. It is known that the error rate due to the noise in the laser heterodyne communication system is

$$BER = Q\left(2\sqrt{\frac{RP_m \sin^2\varphi_{pm}}{R_b q}}\right) \tag{25}$$

where $Q(\cdot)$ is the Q-function defined as[28].

$$Q(\beta) \equiv \frac{1}{\sqrt{2\pi}} \int_{\beta}^{\infty} e^{-\lambda^2/2} d\lambda \tag{26}$$

We can get the theoretical value of *BER* by substituting parameter values in Table 1 into the formula above. If $R_b = 10M$ and $\varphi_{pm} = 3^{\circ}$ (other parameters shown in Table 1, then we can get the bit error rate $BER = 2.44 \times 10^{-9}$). Obviously, the bit error rate is independent of the loop bandwidth from the formula (25). But this does not mean that the loop bandwidth B_n can be any unlimited values. In fact, the phase deviation φ_{pm} created by the phase modulator and the bit error rate R_b are important factors affecting the optimal loop bandwidth. If the loop bandwidth value is not appropriate, the system's phase noise will exceed the system's tolerance, which will lead to an increase in the system's bit error rate.

3.2. The performance of the UHF carrier signal stability

It can be seen from the previous introduction in Section 2.3, the stability of the UHF carrier signal mainly caused by the local

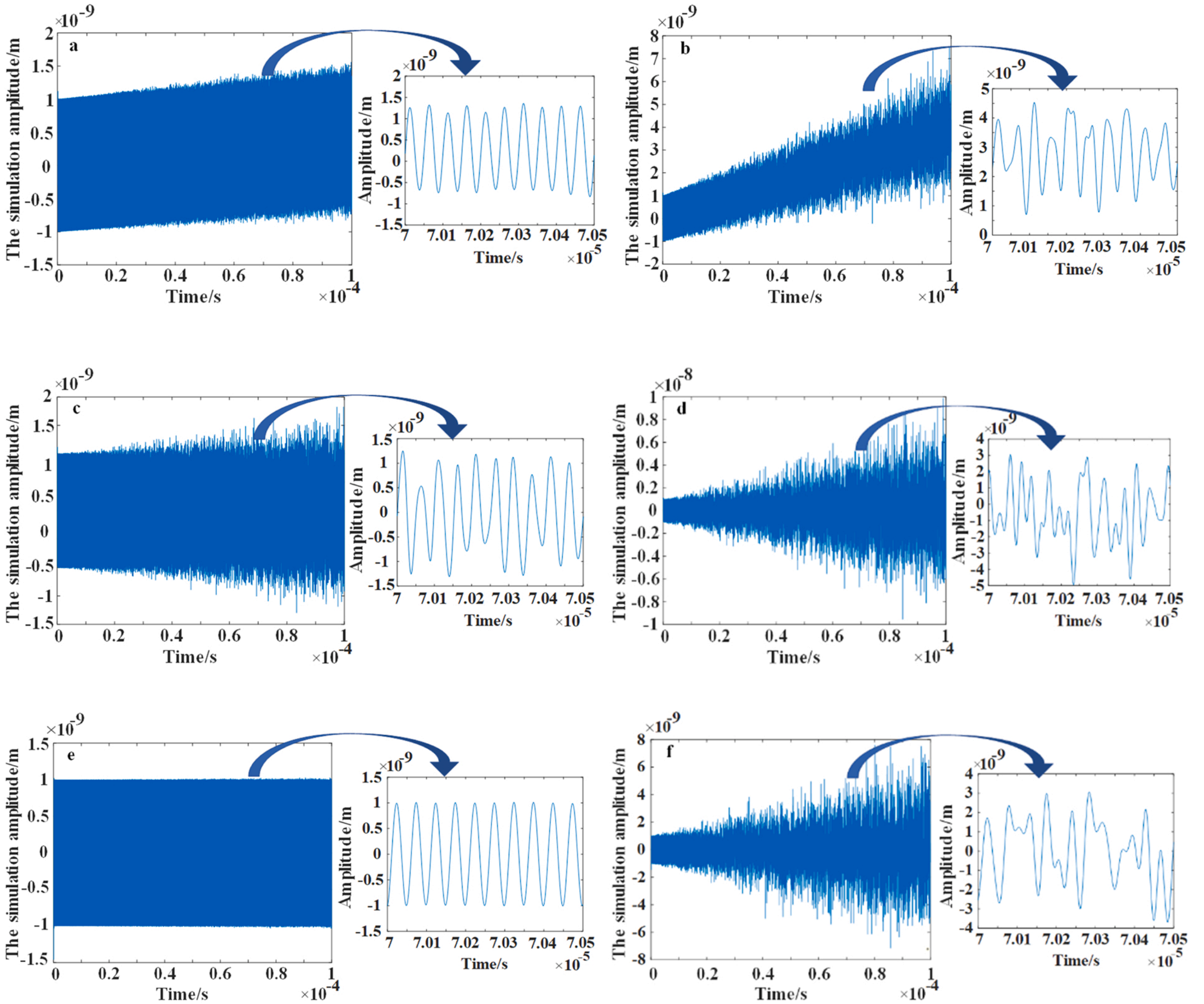

Fig. 7. The time variation curve of the demodulated output signal $s(t)$ with the different random distribution function of the frequency deviation. (a): Random uniform distribution, $f_{ei} = f_{eq} = 10Hz$; (b): Random uniform distribution, $f_{ei} = f_{eq} = 100Hz$; (c): Standard normal distribution, $f_{ei} = f_{eq} = 10Hz$; (d): Standard normal distribution, $f_{ei} = f_{eq} = 100Hz$; (e): Standard normal distribution, $f_{eq} = 0,\ f_{ei} = 100Hz$; (f): Standard normal distribution, $f_{ei} = 0,\ f_{eq} = 100Hz$.

oscillator is the main factor affecting the demodulation accuracy. We will compare the simulation value of the demodulation output phase in the laser heterodyne UHF vibration measurement system with the theoretical value in Eq. (24) to investigate the influence of the frequency and amplitude instability of the carrier signal on the demodulation accuracy. The parameters used in the numerical simulations are given as Table 2. Suppose that the target makes a simple harmonic vibration with a small amplitude:

$$v(t) = \widehat{v}\sin(2\pi f_{vib} t) \tag{27}$$

Sufficient and necessary conditions for the UHF carrier signal stability with constrained control variable are discussed in this section. Through the simulation of the laser heterodyne UHF detection system, time variation curves of the demodulated output signal $s(t)$ with the different random distribution function are shown in Figs. 6 and 7. The precondition for the validity of simulation results is that the OPLL system is assumed to contain only one of the amplitude deviation and frequency deviation and not the other. We assume that the amplitude deviation and frequency deviations obey the random uniform distribution in the interval $[0,\ \Delta U\ or\ f_e]$ or the standard normal distribution with the mean f_c and the variance $\Delta U\ or\ f_e$. From the demodulation results, we can know that the phase generated carrier technique based on the arctangent method can accurately reconstruct the target vibration characteristics when there are no deviations or a small deviation. The demodulation output becomes worse with the increase of the amplitude deviation or the frequency deviation. The probability distribution of the amplitude deviation will also affect the demodulation output, and the standard normal distribution of the amplitude deviation will have greater impact on the demodulation output than the random uniform distribution. Besides, there is a time cumulative error which increases with the time no matter how small the amplitude deviation or the frequency deviation is.

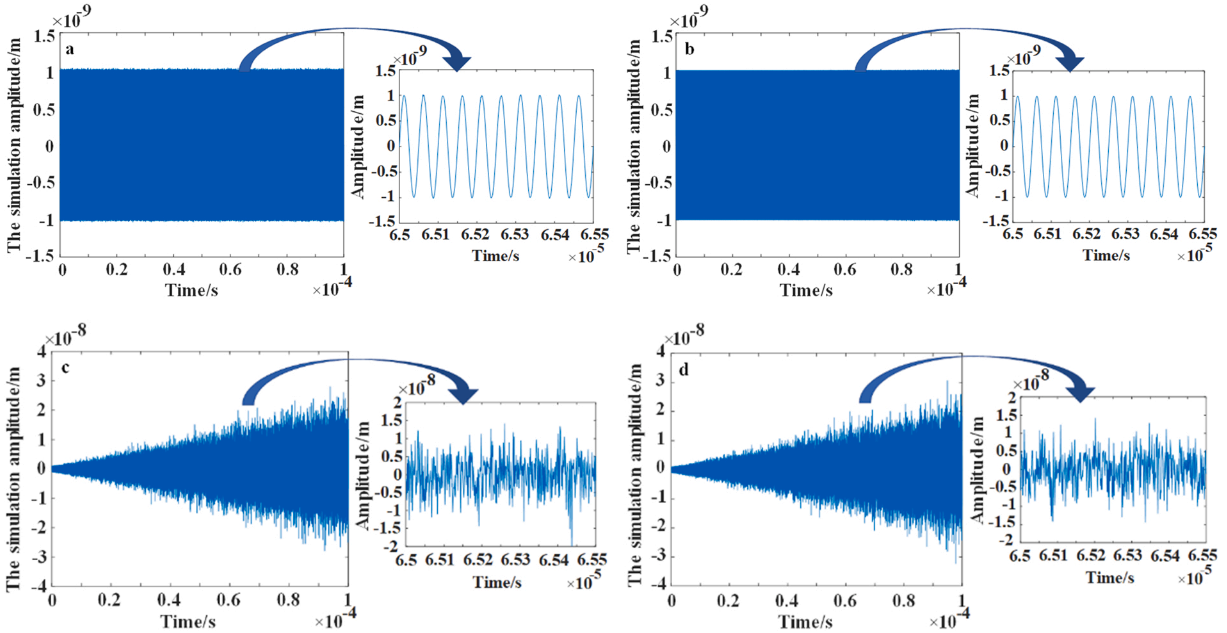

Fig. 8. The theoretical calculated value of demodulated output signal $s_{cal}(t)$ given by the expression (24). (a): $\Delta U/U = 1\times10^{-2}, f_{ei} = f_{eq} = 0$; (b): $\Delta U/U = 0, f_{eq} = 0,\ f_{ei} = 100Hz$; (c): $\Delta U/U = 0, f_{ei} = 0,\ f_{eq} = 100Hz$; (d): $\Delta U/U = 0, f_{ei} = f_{eq} = 100Hz$.

We can recover the theoretical calculated value of demodulated output signal $s_{cal}(t)$ from the calculated phase by $\Delta\varphi_{cal}(t) = \frac{4\pi s_{cal}(t)}{\lambda}$. The theoretical calculated value of demodulated output signal $s_{cal}(t)$ given by the expression (24) is shown in Fig. 8. Through the frequency and amplitude deviations caused by the local oscillator, we numerically analyzed the influence of the instability of the UHF carrier signal on the demodulation accuracy. According to the calculated results, the variation trend of numerical results $s_{cal}(t)$ is consistent with simulated results $s(t)$. And the difference between numerical and simulated results is related to these factors such as laser linewidths of master laser and slave laser, OPLL transfer function and the filter performance of the demodulation process.

Based on above numerical results, we investigate the influence of the residual phase error and the UHF carrier instability on the laser heterodyne UHF detection system. If we want to achieve a high-precision reconstruction of the target vibration, we need to narrow the laser linewidth, reduce the phase deviation created by the phase modulator, increase the system bit rate and select the appropriate loop bandwidth. Besides, the heterodyne-carrier stability mainly controlled by the local oscillator of the OPLL is decisive for the phase demodulation. In other words, we can improve the demodulation accuracy by reducing the frequency and amplitude deviation of the local oscillator.

In contrast to the literature already available[7,8], the numerical analysis findings presented in this article offer a more comprehensive assessment and serve as a quantitative benchmark for evaluating the performance of laser UHF vibration measurement systems. Our research has enhanced the understanding of factors influencing performance in the realm of laser heterodyne UHF vibration measurement and has established a more accurate phase demodulation output model for heterodyne detection systems. Through the establishment of the error gain factor, a comprehensive examination is conducted to assess the influence of residual phase error and carrier stability on laser heterodyne difference detection. Additionally, an alternative is presented to enhance demodulation precision, which can be estimated by the fourth harmonic component in Eq. 24.

4. Conclusion

In summary, the variance of residual phase error and the stability of ultra-high frequency carrier signals have been investigated as a means to characterize the performance of the laser heterodyne detection through a numerical simulation. By utilizing an approximate expression for the variance of residual phase error, the optimization and adjustment of four key factors, namely laser linewidth, noise bandwidth, optical power of the measurement beam, and phase deviation induced by the phase modulator, enable the determination of the minimum value for this variance. Table 1 shows the minimum variance of residual phase error under given conditions and its corresponding minimum loop noise bandwidth.

We proposed a concept of the error gain factor based on the UHF carrier stability, which consists of the amplitude deviation and frequency deviation. We assume that the amplitude deviation follows a uniform random distribution and a standard normal distribution, and discuss the time-variation curve of the demodulation output with amplitude deviations of 1% and 0.1%, frequency deviations of 10 Hz and 100 Hz as simulation parameters. Through comparative analysis of simulation experiments, we found that as long as there is a deviation between two baseband signals, the demodulation output will experience cumulative errors that increase over time, which also verifies the validity of the theoretical analysis.

Furthermore, we propose a high-precision demodulation output model with high-order harmonic components to evaluate the performance of laser heterodyne ultra-high frequency vibration measurement systems. The Taylor series expansion of the error gain function provides a quantitative parameter selection guidance for the higher precision demodulation of laser heterodyne detection. The numerical results suggest that quantitative analysis of laser heterodyne UHF detection performance based on optical phase-locked loops can be achieved through the variance of residual phase error and the deviation of two baseband signals.

Declaration of Competing Interest

The authors declare that they have no known competing financial interests or personal relationships that could have appeared to influence the work reported in this paper.

Data availability

No data was used for the research described in the article.

Acknowledgment

This study is supported by the Natural Science Foundation of Jilin Province (General Program) (20220101116JC) and Youth Fund of the National Natural Science Foundation of China (62305336).

References

[1] D.M. Chen, W.D. Zhu, Investigation of three-dimensional vibration measurement by three scanning laser Doppler vibrometers in a continuously and synchronously scanning mode, J. Sound Vib. 498 (3) (2021), 115950.
[2] L.F. Lyu, W.D. Zhu, Operational modal analysis of a rotating structure under ambient excitation using a tracking continuously scanning laser Doppler vibrometer system, Mech. Syst. Signal Process. 152 (3) (2021), 107367.
[3] Z. Zhang, Y. Wang, H. Zhang, et al., Hypersonic poration: a new versatile cell poration method to enhance cellular uptake using a piezoelectric nano-electromechanical device, Small 13 (18) (2017), 1602962.
[4] Iannacci J., Tschoban C., Reyes J., et al. RF-MEMS for 5G mobile communications: A basic attenuator module demonstrated up to 50 GHz; proceedings of the IEEE Sensors 2016, F, 2017 [C].
[5] Suresh K., Jeoti V., Drieberg M. A read range maximization approach for UWB surface acoustic wave (SAW) RFID tags based on interdigital transducer (IDT) as a reflector. In: Proceedings of the 2020 IEEE 6th World Forum on Internet of Things (WF-IoT), F, 2020 [C].
[6] Y. Nonomura, Sensor technologies for automobiles and robots: Sensor technologies, IEEJ Trans. Electr. Electron. Eng. 15 (2020) 5.
[7] R. Kowarsch, C. Rembe, Heterodyne interferometry at ultra-high frequencies with frequency-offset-locked semiconductor lasers, Meas. Sci. Technol. 31 (7) (2020).
[8] R. Kowarsch, T.E.R. Rembe, Laser-Doppler vibrometer microscope with variable heterodyne carrier, J. Phys. Conf. Ser. 1149 (1) (2018), 012016.
[9] K. Baakier, M.J. Fice, L. Ponnampalam, et al., Foundry fabricated photonic integrated circuit optical phase lock loop, Opt. Express 25 (15) (2017) 16888.
[10] Xin C.A., Xl A., Ys A., et al. Z-domain model procedure for heterodyne digital optical phase-locked loop - ScienceDirect. Optik, 2021.
[11] L.I.U. YANG, ZHAO, et al., Study of multistage composite loop control based on optical phase-locked loop technology, Opt. Commun. 424 (2018) 17–25.
[12] Rembe C., Siegmund G., Steger H., et al. Optical inspection of microsystems. 2007.
[13] Giesen M., Kowarsch R., Ochs W., et al. Optical vibration analysis of MEMS devices with pm-resolution in x, y, and z directions. In: Proceedings of the Optical Measurement Systems for Industrial Inspection VIII, F, 2013 [C]. SPIE.
[14] L.I.Y. Baets r, Nonlinear signal errors in homodyne laser Doppler vibrometry induced by strong second-order ghost reflections and their mitigation, Opt. Express 29 (6) (2021) 8283–8295.
[15] Y. Painchaud, M. Poulin, M. Morin, et al., Performance of balanced detection in a coherent receiver, Opt. Express 17 (5) (2009) 3659–3672.
[16] R. Stierlin, R. B?ttig, P.D. Henchoz, et al., Excess-noise suppression in a fibre-optic balanced heterodyne detection system, Opt. Quantum Electron. 18 (6) (1986) 445–454.
[17] C.H. Yan, T.F. Wang, Y.Y. Li, et al., An improved arctangent algorithm based on phase-locked loop for heterodyne detection system, Chin. Phys. B 28 (3) (2019), 030701.
[18] J. He, L. Wang, F. Li, et al., An ameliorated phase generated carrier demodulation algorithm with low harmonic distortion and high stability, J. Light. Technol. 28 (22) (2010) 3258–3265.
[19] W. Xiao, J. Cheng, D. Zhang, et al., An improved high stability and low distortion phase generated carrier demodulation algorithm for phase-sensitive optical time-domain reflectometers, Laser Phys. Lett. 19 (2022).
[20] Y. Zhu, Z. Wang, K. Tian, et al., Phase-generated carrier combined with the Hilbert transform for phase demodulation in frequency-scanning interferometry, Opt. Lasers Eng. 153 (2022), 106988.
[21] P. Kwee, C. Bogan, K. Danzmann, et al., Stabilized high-power laser system for the gravitational wave detector advanced LIGO, Opt. Express 20 (10) (2012) 10617–10634.
[22] N. Satyan, L. Wei, A. Yariv, Coherence cloning using semiconductor laser optical phase-lock loops, IEEE J. Quantum Electron. 45 (7) (2009) 755–761.
[23] C. Sternkopf, C. Diethold, U. Gerhardt, et al., Heterodyne interferometer laser source with a pair of two phase locked loop coupled He–Ne lasers by 632.8 nm, Meas. Sci. Technol. 23 (7) (2012) 654–657.
[24] J.I. Thorpe, P. Maghami, J. Livas, Time domain simulations of arm locking in LISA, Phys. Rev. D: Part. Fields 83 (12) (2011).
[25] J. Latourrette, S. Jacobs, Heterodyne detection in optical communication techniques, Comput. Meas. Control (1962).
[26] V. Kroupa, Phaselock techniques, Acoust. Speech Signal Process. IEEE Trans. 28 (3) (1980) 349–350.
[27] N. Satyan, J. Sendoski, A. Vasilyev, et al., Phase noise reduction of a semiconductor laser in a composite optical phase-locked loop, Opt. Eng. 49 (12) (2010) 1127–1134.
[28] L.G. Kazovsky, Balanced phase-locked loops for optical homodyne receivers: performance analysis, design considerations, and laser linewidth requirements, J. Light. Technol. 4 (2) (1986) 182–195.
[29] S. Norimatsu, K. Iwashita, PLL propagation delay-time influence on linewidth requirements of optical PSK homodyne detection, J. Light. Technol. 9 (10) (1991) 1367–1375.
[30] L.G. Kazovsky, Decision-driven phase-locked loop for optical homodyne receivers: performance analysis and laser linewidth requirements, IEEE Trans. Electron Devices 32 (12) (1985) 2630–2639.